Supporting Information to accompany

Polyoxotungstate-encapsulated Gd_6 and Yb_{10} complexes

Firasat Hussain,[a] Robert W. Gable,[a] Manfred Speldrich,[b] Paul Kögerler[b] and Colette Boskovic,*[a]

[a] School of Chemistry, University of Melbourne, Victoria, 3010, Australia

[b] Institute of Inorganic Chemistry, RWTH Aachen University, D-52074 Aachen, Germany

Synthesis and Characterization

1: A sample of $Na_9[B\text{-}\alpha\text{-}AsW_9O_{33}]$[1] (0.493 g, 0.200 mmol) was added with stirring to a solution of $Gd(NO_3)_3{\cdot}6H_2O$ (0.271 g, 0.600 mmol) in NaOAc/AcOH buffer (1.0 M, 20 mL) at pH 4.7. This solution was heated to 50 ºC for 30 minutes and then cooled to room temperature, before a small amount of precipitate was removed by filtration. A solution of NH_4Cl (0.027 g, 0.50 mmol) in NaOAc/AcOH buffer (1.0 M, 0.50 mL) at pH 4.7 was added to the filtrate and the resulting solution was left to evaporate. After several weeks the product was obtained as colorless diamond-shaped crystals. The sample for crystallography (**1a**) was maintained in contact with the mother liquor to prevent the loss of interstitial solvent. The bulk sample (**1b**) for further

characterization was obtained by isolating the crystals by filtration, followed by washing them with small quantities of fresh buffer and water and drying them in air. Yield: 0.13 g, 17%. The purity of the bulk sample was confirmed by random unit cell checks and elemental analysis. Single crystal X-ray diffraction gives a formulation of $Na_8H_{30}[Gd_6As_6W_{65}O_{229}(OH)_4(H_2O)_{12}(OAc)_2]\cdot 150H_2O$ for **1a**, with only eight sodium cations and no ammonium cations detected crystallographically due to their small size and crystallographic disorder. However IR peaks at approximately 3300 and 1405 cm^{-1} are consistent with the presence of ammonium cations and nitrogen was evident in the elemental analysis of **1b**. The formulation given below for **1b** is derived from the elemental analysis data obtained for the dried sample. Elemental analysis (%) calcd for $Na_{27}(NH_4)_2H_9[Gd_6As_6W_{65}O_{229}(OH)_4(H_2O)_{12}(OAc)_2]\cdot 35H_2O$ (**1b**, $C_4H_{121}N_2O_{284}As_6Gd_6Na_{27}W_{65}$): C, 0.26; H, 0.65; N, 0.15, Na, 3.32; W, 63.89. Found: C, 0.10; H, 1.09; N, 0.11, Na, 3.30; W, 59.90. Thermogravimetric analysis was consistent with the loss of 35 H_2O molecules of solvation for the air-dried sample **1b**, indicating that some of the water molecules that are present in the wet crystal are lost upon air-drying**.** Selected IR data (KBr disk, cm^{-1}): 950(s), 865(vs), 790(s), 724(m), 639(sh), 478(m).

2: A sample of $Na_9[B\text{-}\alpha\text{-}AsW_9O_{33}]$ (0.493 g, 0.200 mmol) was added with stirring to a solution of $YbCl_3\cdot 6H_2O$ (0.233 g, 0.600 mmol) in NaOAc/AcOH buffer (1.0 M, 20 mL) at pH 4.7. This solution was heated to 50 ºC for 30 minutes and then left overnight to cool and for any precipitate to settle. A small amount of precipitate was removed by filtration and a solution of CsCl (0.021 g, 0.13 mmol) in NaOAc/AcOH buffer (1.0 M, 0.25 mL) at pH 4.7 was added to the filtrate and the resulting solution was left to evaporate. After several weeks the product was obtained as colorless rod-shaped crystals.

The sample for crystallography (**2a**) was maintained in contact with the mother liquor to prevent the loss of interstitial solvent. The bulk sample (**2b**) for further characterization was obtained by isolating the crystals by filtration, followed by washing them with small quantities of fresh buffer and water and drying them in air. Yield: 0.11 g, 15%. The purity of the bulk sample was confirmed by random unit cell checks and elemental analysis. Single crystal X-ray diffraction gives a formulation of $Na_{15.69}Cs_{15.31}H_9[Yb_{10}As_{10}W_{88}O_{308}(OH)_8(H_2O)_{28}(OAc)_4]\cdot 84H_2O$ for **2a**, with crystallographic disorder of the cations preventing detection of all the sodium and cesium cations. The formulation given below for **2b** is derived from the elemental analysis data obtained for the dried sample. Elemental analysis (%) calcd for $Na_{28}Cs_{12}[Yb_{10}As_{10}W_{88}O_{308}(OH)_8(H_2O)_{28}(OAc)_4]\cdot 84H_2O$ (**2b**, $C_8H_{244}O_{436}As_{10}Cs_{12}Na_{28}W_{88}Yb_{10}$): Cs, 5.65; Na, 2.28; W, 57.34; Yb, 6.13; As, 2.66. Found: Cs, 5.3; Na, 2.7; W, 57.0; Yb, 5.0; As, 2.4. Selected IR data (KBr disk, cm^{-1}): 949(s), 870(vs), 783(s), 715(m), 641(sh), 590 (sh), 484(m).

X-ray Crystallography

Crystal data for **1a** ($C_4H_{131.07}As_6Gd_6Na_8O_{398.07}W_{65}$; M = 20076.38): triclinic, space group *P-1*, a = 23.0942(17), b = 25.6844(18), c = 31.749(3) Å, α = 66.2300(10), β = 83.185(2), γ = 84.002(2)°, V = 17080(2) $Å^3$, Z = 2, T = 130(2) K, ρ = 3.904 gcm^{-3}, $\mu(Mo_{K\alpha})$ = 23.655 mm^{-1}. A colorless block with dimension of 0.13 × 0.10 × 0.06 mm^3 was mounted in a Hamptom cryoloop for indexing and intensity data collection at 130 K(2) on a Bruker Smart CCD single- crystal diffractometer ($Mo_{K\alpha}$ radiation, λ = 0.71073 Å).Of the 90156 reflections collected ($2\theta_{max}$ = 50.06, 95.3% complete), 59424 were

unique (R_{int}= 0.074) and 34275 reflections were considered observed ($I > 2\sigma(I)$). Routine Lorentz and polarization corrections were applied, and an absorption correction was performed using the SADABS program.[2] Direct methods were used to locate the tungsten and gadolinium atoms (SHELXS-97). Then the remaining atoms were found from successive Fourier maps (SHELXL-97). The final cycle of refinement, including the atomic coordinates, anisotropic thermal parameters (W, As, Gd atoms), and isotropic thermal parameters (O and Na atoms) converged at R = 0.066 ($I > 2\sigma(I)$) and R_w = 0.162 (all data). In the final difference map the deepest hole was –2.72 eÅ^{-3} and the highest peak 3.00 eÅ^{-3}.

Crystal data for **2a** ($C_8H_{253}As_{10}Cs_{15.31}Na_{15.69}O_{436}W_{88}Yb_{10}$; M_r = 28381.07 g mol^{-1}): triclinic, space group *P-1*, a = 21.476(3), b = 24.164(3), c = 27.725(4) Å, α = 70.632(2), β = 70.009(2), γ = 76.675(3)°, V = 12644(3) Å^3, Z = 1, T = 130(2) K, ρ = 3.727 g cm^{-3}, $\mu(Mo_{K\alpha})$ = 23.598 mm^{-1}. A colorless plate with dimension of 0.29 × 0.09 × 0.03 mm^3 was mounted in a Hampton cryoloop for indexing and intensity data collection and structure solution and refinement was as for **1a**. Of the 67318 reflections collected ($2\theta_{max}$ = 50.06, 98.6% complete), 44054 were unique (R_{int} = 0.077) and 27391 reflections were considered observed ($I > 2\sigma(I)$). The final cycle of refinement, including the atomic coordinates, anisotropic thermal parameters (W, As, Yb and Cs atoms), and isotropic thermal parameters (O and Na atoms) converged at R = 0.094 ($I > 2\sigma(I)$) and R_w = 0.254 (all data). In the final difference map the deepest hole was –5.63 eÅ^{-3} and the highest peak 6.43 eÅ^{-3}.

CCDC 678641 (**1a**) and 678642 (**2a**) contains the supplementary crystallographic data for this paper. These data can be obtained free of charge from the Cambridge Crystallographic Data Centre via www.ccdc.cam.ac.uk/data-request/cif.

Magnetic Measurements

Magnetic susceptibility measurements were performed at 0.1 Tesla in a temperature interval of 2–290 K using a Quantum Design MPMS-5XL SQUID magnetometer. The experimental susceptibility values were corrected for diamagnetic and temperature-independent paramagnetic (TIP) contributions ($\chi_{dia/TIP}$(**1b**) = -1.69×10^{-3} emu mol^{-1}; $\chi_{dia/TIP}$(**2b**) = -2.32×10^{-3} emu mol^{-1}). Note that these values are calculated from both tabulated values and from experimentally derived values for diamagnetic {AsW_9O_{33}}-type compounds.

Theoretical modeling: We consider a magnetically isolated f^N metal ion surrounded by ligands imposing a distinct point symmetry upon the magnetic center. In a static magnetic field ***B*** the Hamiltonian of the metal ion is then represented

by

$$\hat{H} = \underbrace{\sum_{i=1}^{N}\left[-\frac{\hbar^2}{2m_e}\nabla_i^2 + V(r_i)\right]}_{\hat{H}^{(0)}} + \underbrace{\sum_{i>j}^{N}\frac{e^2}{r_{ij}}}_{\hat{H}_{\mathrm{ee}}} + \underbrace{\sum_{i=1}^{N}\zeta(r_i)\,\kappa\;\hat{\boldsymbol{l}}_i\cdot\;\hat{\boldsymbol{s}}_i}_{\hat{H}_{\mathrm{so}}} + \tag{1}$$

$$\underbrace{\sum_{i=1}^{N}\sum_{k=0}^{\infty}\left\{B_0^k C_0^k(i) + \sum_{q=2}^{k}\left[B_q^k\left(C_{-q}^k(i) + (-1)^q C_q^k(i)\right)\right]\right\}}_{\hat{H}_{\mathrm{LF}}} +$$

$$\underbrace{\sum_{i=1}^{N}\mu_B(\kappa\;\hat{\boldsymbol{l}}_i + 2\;\hat{\boldsymbol{s}}_i)\cdot\;\boldsymbol{B}}_{\hat{H}_{\mathrm{mag}}}$$

While $H^{(0)}$ represents the energy in the central field approximation, H_{ee} and H_{so} account for interelectronic repulsion and spin-orbit coupling (modified by the orbital reduction factor κ), respectively. The former is taken into account by the Slater-Condon parameters F^2, F^4, F^6, the latter by the one-electron spin-orbit coupling parameter ζ. These sets of interelectronic repulsion parameters as well as ζ and κ are used as constants in the fitting calculations.

H_{LF} accounts for the electrostatic effect of the ligands (within the ligand field theory framework) on the basis of the global parameters B^k_q. The summation i is carried out over all N f-electrons. The spherical tensors C^k_q are directly related to the spherical harmonics ($C_q^k = \sqrt{4\pi/(2k+1)}Y_q^k$) and the real ligand field parameters B^k_q (Wybourne notation)[3,4] are given by $A_k^q\left\langle r^k\right\rangle$ where A^q_k is a numerical constant characterizing the charge distribution in the environment of the metal ion and $\langle r^k\rangle$ is the expectation value of r^k. For f electrons the terms in the expansion with $k \leq 6$ are nonzero, whereas all terms with odd k values vanish since we consider only configurations containing equivalent

electrons. The values of k and q are limited by the point symmetry of the metal ion site. If the spherically symmetric term $B^0{}_0\, C^0{}_0$ (which does not cause any splitting) is ignored, in cubic systems only spherical tensors with $k = 4$ and $k = 6$ are relevant and all $B^k{}_q$ are zero. The ligand field operator with reference to the fourfold rotation axis for the angular part of the wave function reads

$$H_{LF}^{tet} = B_0^2 \sum_{i=1}^{N} C_0^2(i) + B_0^4 \sum_{i=1}^{N} \left[C_0^4(i) + \sqrt{5/14}\left(C_4^4(i) + C_{-4}^4(i)\right)\right] + B_0^6 \sum_{i=1}^{N} \left[C_0^6(i) - \sqrt{7/2}\left(C_4^6(i) + C_{-4}^6(i)\right)\right]$$

Therefore, the following parameters have been used to fit the observed susceptibility data: the one-electron spin-orbit coupling constant ζ and the set of ligand field parameters $B_0{}^2$, $B_0{}^4$, $B_4{}^4$, $B_0{}^6$, and $B_4{}^6$ for the tetragonal local environment.

For magnetochemical analyses the program CONDON was used.[5] For modeling the magnetic behaviour of the $4f^{13}$-system (**1**) LF effects $\left(H_{\mathrm{LF}}\right)$ and spin-orbit-coupling $\left(H_{\mathrm{so}}\right)$ have to be taken into account. Especially important is the consideration of H_{LF}. To reduce the number of LF parameters, the local point symmetry was idealized to D_{4h}. The initial set of B_q^k parameter values were taken from spectroscopically determined energy levels for Yb(III) in cubic elpasolite crystals.[6] In order to determine the corresponding ligand field parameters B_q^k the assumption of D_{4h} symmetry was sufficient to yield an excellent fit (Figure 4, SQ = 0.43%) for $B_0{}^2 = 538$ cm^{-1}, $B_0{}^4 = 1890$ cm^{-1}, and $B_0{}^6 = -24$ cm^{-1}. The fitting procedure employed:

(1) As starting parameters for a cubic Yb^{3+} system ($B_0{}^4$ and $B_0{}^6$) the values for the corresponding compound listed in ref. 6.

(2) The ratios between the parameters B_0^4 and B_4^4 as well as B_0^6 and B_4^6 were set as constant, reflecting cubic ligand field symmetry ($B_0^4 / B_4^4 = (5/14)^{1/2}$; $B_0^6 / B_4^6 = -(7/2)^{1/2}$).[4] Note that the quality of the fit does not increase significantly upon removing these constraints.

(3) To accommodate the assumed near-tetragonal symmetry of the Yb^{3+} ligand field, a third free parameter B_0^2 was introduced.

(4) The (fixed) spin-orbit coupling parameter was chosen as $\zeta = 2904\ cm^{-1}$ according to ref. 6.

Other Measurements

Infrared spectra (KBr disk) were recorded on a BioRad 175 FTIR spectrometer. Elemental analyses were performed by Chemical and Microanalytical Services, Belmont, Victoria, Australia and Zentrale Chemische Analytik (ZCH), Forschungszentrum Jülich, D-52425 Jülich, Germany.

References

1 C. Tourné, A. Revel, G. Tourné and M. Vendrall, *C. R. Acad. Sci. Paris, Ser. C* 1973, **277**, 643.

2 G. M. Sheldrick, Siemens Analytical X-ray Instrument Division: Madison, WI, 1995

3 B. G. Wybourne, *Spectroscopic Properties of Rare Earths*, Wiley, New York **1965**.

4 C. Görller-Walrand and K. Binnemans, *Rationalization of crystal-field parametrization*, in: K. A. Gschneidner, Jr., L. Eyring (Eds.), *Handbook on the Physics and Chemistry of Rare Earths*, Vol. **23**, Ch. 155, p. 121, Elsevier, Amsterdam 1996.

5 H. Schilder and H. Lueken, *J. Magn. Magn. Mater.* 2004, **281**, 17.

6 P. A. Tanner, V. V. Ravi Kanth Kumar, C. K. Jayasankar and M. F. Reid, *J. Alloys and Compounds* 1994, **215**, 349.

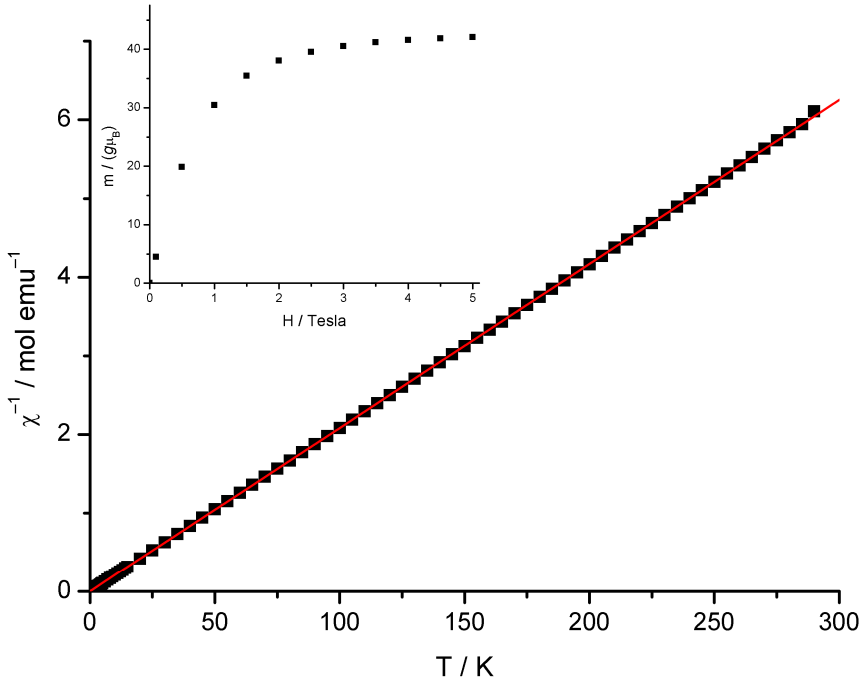

Fig. S1. Temperature dependence of the reciprocal susceptibility of **1b** at 0.1 Tesla emphasizing the near perfect Curie paramagnetism (black squares: experimental data, red line: least-squares linear fit). Inset: Magnetization as a function of external field at 2.0 K, showing a Brillouin-type behavior.